

# Exact results for the Barabási queuing model

C. Anteneodo

*Departamento de Física, PUC-Rio and National Institute of Science and Technology for Complex Systems,  
Rua Marquês de São Vicente 225, CEP 22453-900 RJ, Rio de Janeiro, Brazil*

Previous works on the queuing model introduced by Barabási to account for the heavy tailed distributions of the temporal patterns found in many human activities mainly concentrate on the extremal dynamics case and on lists of only two items. Here we obtain exact results for the general case with arbitrary values of the list length  $L$  and of the degree of randomness that interpolates between the deterministic and purely random limits. The statistically fundamental quantities are extracted from the solution of master equations. From this analysis, new scaling features of the model are uncovered.

PACS numbers: 89.75.Da 89.75.-k, 02.50.Le

## I. INTRODUCTION

Many human activities, such as mail and e-mail exchanges, library loans, stock market transactions [1], or even motor activities [2], display heavy tailed inter-event and waiting time distributions. To account for these heavy tails [1], a priority queuing model has been proposed by Barabási [3], that since then stimulated an active field of research with potential practical applications (e.g., see Refs. [4, 5, 6, 7, 8]).

Within Barabási priority queuing model (BQM), each item in a list of fixed length  $L$  has a priority value. At each time-step, the maximal priority task is executed with probability  $p$ , otherwise, a randomly selected one is accomplished. Once a task is executed, it is substituted by a new one (or the same) that adopts a new randomly selected priority value drawn from a probability density function (PDF)  $\rho(x)$ . This simple model yields power-law tailed distributions of inter-events times, mimicking the empirical histograms of many human activities.

Besides the value of queuing models for diverse practical questions, another issue that makes BQM attractive is its connection with diverse other physical problems such as invasion percolation [8, 9] or self-organized evolutionary models [10, 11, 12], as soon as the roles of priorities and fitness can be identified.

However, exact results for the BQM, both for steady [6] and transient [8] regimes, have been obtained for the simplest instance  $L = 2$  only. Although lists of two items already display the power-law decay of the distribution of waiting times when  $p$  approaches unity, naturally, other features are missed in the simplest case. Moreover, special attention has been given to the particular, and more tractable case, of extremal dynamics when  $p \rightarrow 1$  [1, 5, 9], while non-null degree of randomness ( $1 - p \neq 0$ ) may also display interesting features. Then, in the present work, we tackle the BQM with arbitrary values of  $p$  and  $L$ .

The manuscript is organized as follows. In the next section we show exact results for the PDFs of priorities in lists of arbitrary length  $L$ , by recourse to a master equation. In Sec. III we obtain an approximate expression for the waiting time distribution. Sec. IV deals with ex-

act results for “avalanches” which provide the time that higher priority tasks (above a threshold) remain in the list, and is also related to waiting time duration. The last section contains final remarks.

## II. EXACT TREATMENT

A fundamental quantity is the probability that there are  $n$  tasks with priority higher than a given value  $x$ , at time  $t$ ,  $P_{n,t}(x)$ . Its time evolution is ruled by a master equation (ME) of the form

$$P_{n,t+1} = M_{n,n+1}P_{n+1,t} + M_{n,n}P_{n,t} + M_{n,n-1}P_{n-1,t}, \quad (1)$$

for  $n = 0, 1, \dots, L$ , with the non-null elements of the tridiagonal matrix  $\mathbf{M}$  given by

$$\begin{aligned} M_{n-1,n}(x) &= px + (1-p)xn/L, \\ M_{n,n}(x) &= p(1-x) + (1-p)(x(L-n) + (1-x)n)/L, \\ M_{n+1,n}(x) &= (1-p)(1-x)(L-n)/L, \end{aligned} \quad (2)$$

for  $n = 1, \dots, L$ , and additionally  $M_{1,0}(x) = 1 - x$ ,  $M_{0,0}(x) = x$ . Here we have taken  $\rho(x) = 1$ , however generality can be recovered simply by redefining the threshold through  $x \rightarrow R(x) = \int_0^x \rho(x')dx'$ .

Notice that the ME (1)-(2) signals a biased random walk with reflecting boundaries at  $n = 0$  and  $n = L$ , setting the basis to write a continuum limit approximation. However, for arbitrary  $L$ , drift and diffusion coefficients are state dependent and the approach of biased diffusion successfully applied [5] to determine the scaling of the waiting time distribution, in other queuing systems with constant coefficients, becomes more tricky in the non-deterministic case  $p \neq 1$ .

Then, let us find the exact steady solution of the ME (1)-(2) for arbitrary length  $L$ . By recursion, one gets

$$P_n(x) = \frac{L!\Gamma(a+1)(1-x)^n}{(L-n)!\Gamma(a+n+1)(1-p)x^n} P_0(x), \quad (3)$$

for  $1 \leq n \leq L$ , where  $a = pL/(1-p)$ , and from normalization

$$P_0(x) = \left(1 + \sum_{n=1}^L P_n(x)/P_0(x)\right)^{-1}. \quad (4)$$

The distribution  $P_n$ , given by Eqs. (3)-(4), can be used now to evaluate diverse meaningful quantities. In particular, the PDF of the  $n$ th largest priority value can be extracted from the condition  $\int_0^x p_n(x')dx' = \sum_{m=0}^{n-1} P_m(x)$ , hence

$$p_n(x) = \frac{\partial}{\partial x} \sum_{m=0}^{n-1} P_m(x). \quad (5)$$

Fig. 1 shows the exact PDFs of the two largest priorities in the list,  $p_1(x) = P'_0(x)$  and  $p_2(x) = P'_0(x) + P'_1(x)$ , for  $L = 5$  and different values of  $p$ , compared to the results of numerical simulations of the BQM.

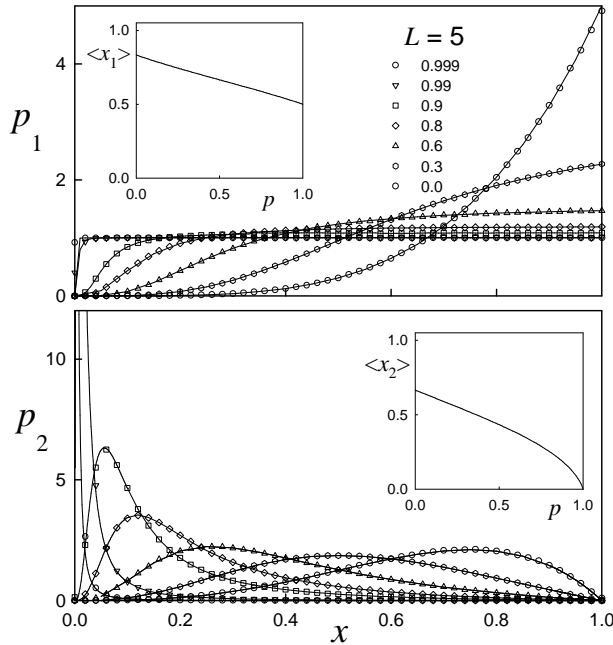


FIG. 1: PDFs of the largest (upper panel) and the second largest (lower panel) priority values, for  $L = 5$ , different values of  $p$  indicated on the figure and  $R(x) = x$ . Solid lines correspond to exact results and symbols to numerical simulations of the BQM performed as in previous figures. In the insets, the average values are displayed as a function of  $p$ .

In the fully random case  $p = 0$ , Eqs. (3)-(4) yield  $P_n(x) = \binom{L}{n}(1-x)^n x^{L-n}$ , hence  $p_n(x) = L \binom{L-1}{n-1} (1-x)^{n-1} x^{L-n}$ , in accord with straightforward combinatorial analysis. In the opposite limit  $p \rightarrow 1$ ,  $p_1(x)$  gets closer to a unit step function at  $x = 0$  while  $p_2(x)$  approaches the Dirac delta function  $\delta(x)$ . This is expected since those tasks that have entered the list more recently and adopted priority values uniformly distributed in  $[0,1]$  have more chances to be chosen again, while the older tasks are more and more likely to remain in the list forever as  $p$  tends to 1, then the second priority value (and together with it the remaining ones) collapse to zero.

For large enough  $L$  (namely,  $L/(1-p) \gg 1$ ), Eqs. (3)-(4) lead to  $p_1 \simeq H(x-1+p)/p$ , where  $H$  is the Heaviside

unit step function, and  $p_2 \simeq (1-p)(1/x^2 - 1)H(x-1+p)/p^2$ . In fact, finding directly the steady state solution of the ME (1)-(2), in the limit of large  $L$  for fixed  $n$  (hence neglecting terms of order  $n/L$ ), or also when  $p \rightarrow 1$ , one obtains a geometric progression that, for  $x > 1-p$ , can be summed up to obtain the simple expression

$$P_0(x) \simeq (x-1+p)/p \quad \text{and} \quad (6)$$

$$P_n(x) \simeq \frac{(x-1+p)(1-p)^{n-1}(1-x)^n}{p^{n+1}x^n}, \quad \text{for } 0 < n \leq L. \quad (7)$$

For  $x \leq 1-p$ , all  $P_n$  tend to vanish in the large  $L$  limit. Fig. 2 illustrates the performance of this approximation in comparison with exact results. The assumption  $n \ll L$  fails as soon as the probability that  $n > \mathcal{O}(1)$  becomes non negligible. For each  $x < 1-p$ , the exact  $P_n$  is peaked around  $n \simeq (x-1+p)L/(1-p)$ . The approximation becomes exact both in the limits of  $L \rightarrow \infty$  and  $p \rightarrow 1$ .

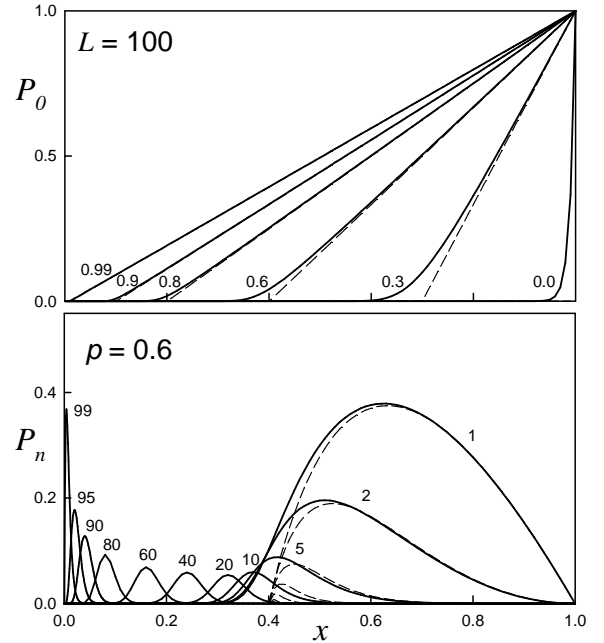


FIG. 2: Probabilities  $P_0(x)$  (for different values of  $p$ , upper panel) and  $P_n(x)$  (for different values of  $n$  and  $p = 0.6$ , lower panel), at  $L = 100$  and  $R(x) = x$ . Solid lines correspond to exact results, dashed lines to the large  $L/(1-p)$  approximation.

The PDF of all priorities  $x$  in the list,  $p(x)$  verifies  $\sum_{n=1}^L p_n(x) = Lp(x)$ . Its time evolution is given by

$$p(x, t+1) = p(x, t) + (\rho(x) - pp_1(x, t) - (1-p)p(x, t))/L, \quad (8)$$

that in the long-time limit leads to the relation

$$pP_0(x) + (1-p)P(x) = R(x), \quad (9)$$

where  $P(x) = \int_0^x p(x')dx'$ .

Let us call old tasks those items whose priority has not been assigned at a given step. The cumulative PDF of old task priorities,  $O(x)$ , can be obtained from the relation

$$LP(x) = R(x) + (L-1)O(x) \quad (10)$$

and, by means of Eq. (9) can be expressed as

$$O(x) = \frac{(L+p-1)R(x) - pLP_0(x)}{(L-1)(1-p)}. \quad (11)$$

In the particular case  $L = 2$ , Eqs. (3)-(4) give  $P_0(x) = (1+p)x^2/(1-p+2px)$  and recalling that its derivation was carried out for uniform  $\rho(x)$  but the general case is recovered simply through the mapping  $x \rightarrow R(x)$ , then, Eq. (11) allows to re-obtain the result of Vazquez [6], namely,  $O(x) = (1+p)R(x)/[1-p+2pR(x)]$ .

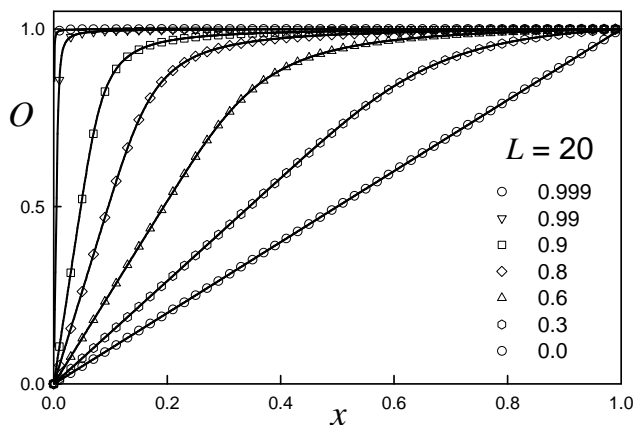


FIG. 3: Cumulative PDFs of old task priorities, for  $L = 20$ , different values of  $p$  and  $R(x) = x$ . Symbols correspond to numerical simulations of the BQM performed as in previous figures, black lines to the exact results from Eq. (11).

Fig. 3 illustrates the behavior of  $O(x)$  for different values of  $p$  and  $L = 20$ . The distribution of the bulk of old values for arbitrary  $L$  is qualitatively similar to that obtained for  $L = 2$  in Ref. [6].

For  $L > 2$ , however,  $P(x)$  and  $O(x)$  are mean-field quantities, while more meaningful is the distribution of the largest old priority  $O_1(x)$  (that, of course, for  $L = 2$  coincides with  $O(x)$ ). It verifies

$$P_0(x) = R(x)O_1(x), \quad (12)$$

since the probability that there are no tasks above  $x$ ,  $P_0(x)$ , is the product of the probability that the freshly assigned (new) priority value is below  $x$  times the probability that the highest old task priority (hence also the remaining ones) is below  $x$ , as soon as the new priority value and the old ones are independent. For the particular case  $p = 0$ ,  $O_1(x) = R^{L-1}(x)$  while in the opposite limit  $p \rightarrow 1$ , it tends to a unit step function at  $x = 0$ .

For  $L > 2$ , the distribution of the second largest old priority  $O_2(x)$  can be extracted from the identity

$$P_1 = (1-R)O_1 + R(O_2 - O_1), \quad (13)$$

which comes from considering that the probability that there is only one task above  $x$ ,  $P_1(x)$ , is  $\text{prob.}[\text{new} \geq x \wedge \text{1st old} \leq x] + \text{prob.}[\text{new} \leq x \wedge \text{2nd old} \leq x \wedge \text{1st old} \geq x]$ , while  $\text{prob.}(\text{2nd old} \leq x \wedge \text{1st old} \geq x) = \text{prob.}(\text{2nd old} \leq x) - \text{prob.}(\text{2nd old} \leq x \wedge \text{1st old} \leq x) = O_2(x) - O_1(x)$ , since the first and second largest old values are not independent. Analogously, in general one has

$$P_n = (1-R)(O_n - O_{n-1}) + R(O_{n+1} - O_n), \quad (14)$$

for  $1 \leq n \leq L-1$ , taking  $O_0 = 0$  and  $O_L = 1$ , while  $P_L = (1-R)(1 - O_{L-1})$ . From where the whole family of stationary old task distributions can be straightforwardly obtained.

Exact results for  $O_1(x)$  and  $O_2(x)$  are compared to the outcomes of numerical simulations of the BQM in Fig. 4, for  $L = 20$ , different values of  $p$  and  $R(x) = x$ . Observe that  $O_2(x)$  is bounded from below by  $O_1(x)$  and more generally  $O_1(x) \leq O_2(x) \leq \dots \leq O_{L-1}(x)$ .

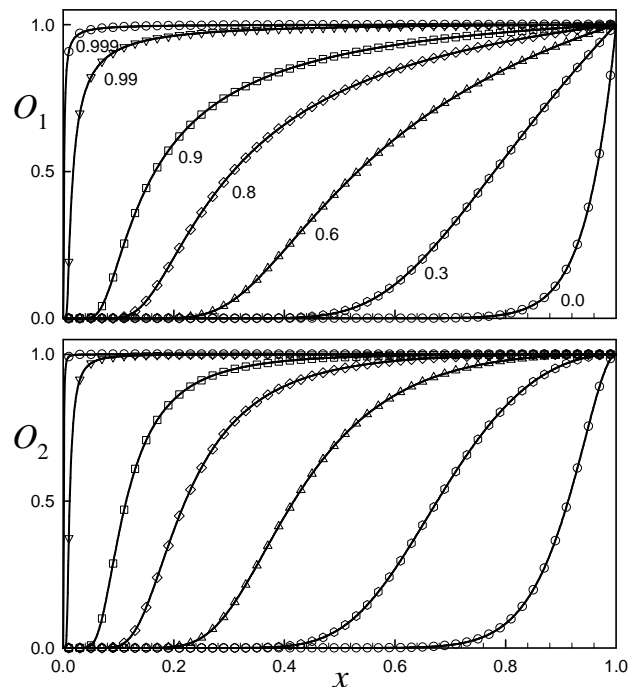


FIG. 4: Cumulative PDFs of the first (upper panel) and second (lower panel) largest old task priorities, for  $L = 20$ , different values of  $p$  and  $R(x) = x$ . Symbols correspond to numerical simulations of the BQM performed as in previous figures, black lines to the exact results from Eqs. (12)-(13).

### III. WAITING TIME DISTRIBUTION

The family of distributions of old values  $\{O_n, 1 \leq n \leq L-1\}$  should in principle allow to compute exactly the distribution of waiting times  $P_w(\tau)$  in the steady regime.

$P_w(\tau)$  can be obtained as

$$P_w(\tau) = \int_0^1 dR(x)r_\tau(x), \quad (15)$$

where  $r_\tau(x)$  is the probability that a task (let us call it  $X$ ) with freshly acquired priority value  $x$  at a given time  $t = t_0$  (once attained the steady state) is again selected for the first time at  $t = t_0 + \tau$ .

For  $\tau = 1$ ,

$$r_1(x) = pO_1(x) + (1-p)/L. \quad (16)$$

Hence  $P_w(1) = 1/L$  when  $p = 0$  and it tends to one in the opposite case  $p \rightarrow 1$ . By means of the approximate Eq. (6) for  $P_0(x)$ , one has  $P_w(1) \simeq p + (1-p)\ln(1-p) + (1-p)/L$ .

The probability that, instead of  $X$ , the first old task is selected at  $t_0 + 1$  is  $p(1 - O_1(x)) + (1-p)/L$ , while the probability that any other old task is selected (for  $L > 2$ ) is  $(1-p)/L$ . Given each of these  $L-1$  cases, for computing  $r_2(x)$ , one has in principle a different probability of selection of  $X$  at the second step ( $t = t_0 + 2$ ) which will be a function of  $O_1$  and  $O_2$ . More generally, the exact calculation of  $P_w(\tau)$ , for  $\tau > 1$ , will require to consider a branching process, with  $L-1$  paths at each node, such that for  $L > 2$ ,  $r_\tau(x)$  does not factorize. This tree generalizes the branching process considered in analogy to invasion percolation for  $L = 2$  [8].

In the first steps (up to  $\tau \sim L$ ), the statistics will be conditioned by the memory of previous selections (aging regime). This is because recently chosen tasks have propensity (the higher, the closer  $p$  to 1) to be chosen again, dominating  $P_w$  at small  $\tau$ .

In particular, for  $\tau = 2$  one obtains

$$r_2(x) = c(1-r_1) + pR[(p+c)O_2 + \{c(L-2)-p\}O_1], \quad (17)$$

where  $c = (1-p)/L$ . For the special case  $L = 2$ ,  $O_2 = 1$ , then one recovers the expression found in Ref. [6] for  $L = 2$ , namely,  $r_2 = (1-r_1)[pR + (1-p)/2]$ .

At further time-steps this is a hard trail to proceed and the results may not be expressible in a readily manageable form. However, notice that while for small  $\tau$ , the integral of  $r_k$  is dominated by large values of  $x$ , due to the propensity of such values to be re-chosen early, contrarily, for large enough  $\tau$ ,  $r_\tau$  (and hence  $P_w$ ) will gain the main contribution from the purely random (unconditioned) selection from the bulk of relatively small  $x$  values (as can be seen in Fig. 5 where  $r_\tau(x)$  is displayed). This is expected to apply also when  $p \rightarrow 1$  at any  $\tau$ . For such cases, one can write

$$r_\tau(x) \simeq (1-r_1(x))(1-f(x))^{\tau-2}f(x), \quad (18)$$

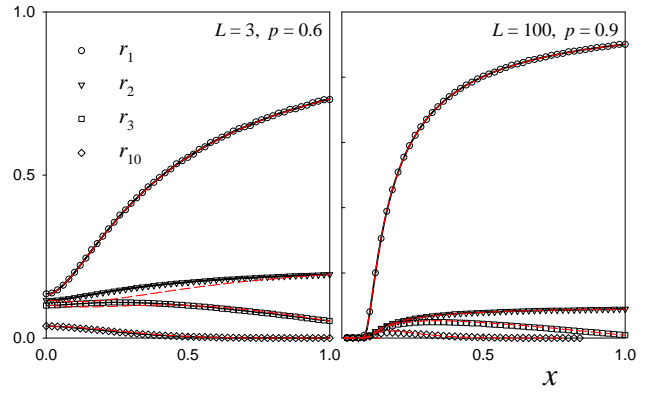


FIG. 5: (Color online) Integrands  $r_\tau$  of the distribution of waiting times, for values of  $\tau$  indicated on the figure and two couples of parameters  $(L, p)$ . Symbols correspond to numerical simulations, solid lines to exact results and dashed red lines to the approximate analytical expressions.

where  $f(x)$  is the effective probability that task  $X$  is selected at some given step  $t > t_0 + 1$  and can be estimated as  $f(x) = pP_0(x) + (1-p)/L$ , as soon as  $P_0 = RO_1$  is the probability that there are no tasks with priorities higher than  $x$ . Fig. 5 also exhibits the comparison between exact

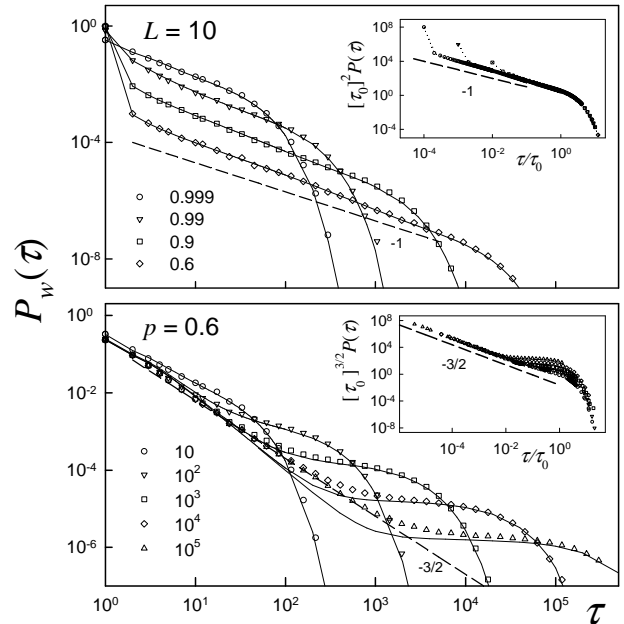


FIG. 6: Distributions of waiting times, for fixed size  $L = 10$  and different values of  $p$  indicated on the figure (upper panel) and for fixed  $p = 0.6$  and increasing values of  $L$  indicated on the figure (lower panel),  $R(x) = x$ . Solid lines join the analytical results from Eqs. (15) and (18) and symbols correspond to numerical simulations of the BQM. Insets: rescaled plots of the numerical histograms, where  $\tau_0 = 1/\ln(L/(L-1+p))$ . Dashed lines with slopes  $-1$  (upper inset) and  $-3/2$  (lower inset) are drawn for comparison.

and approximated functions  $r_\tau$ .

In particular, for  $p = 0$ , Eq. (15) is independent of the choice of  $f(x)$  and it correctly yields the pure exponential decay  $P_w(\tau) = (1 - 1/L)\tau^{-1}/L$  for all  $\tau$  [3]. In the opposite case  $p \rightarrow 1$ , and using the approximation given by Eq. (6) for  $P_0$ , Eq. (15) leads to the asymptotic behavior

$$P_w(\tau) \sim \frac{1}{\tau} \exp(-\tau/\tau_0), \quad (19)$$

where  $\tau_0 = 1/\ln(L/(L - 1 + p)) \sim L/(1 - p)$ .

This expression for the characteristic time  $\tau_0$  applies for any  $p$ . Thus, the characteristic exponential decay time  $\tau_0$  is shifted to larger  $\tau$  when  $p \rightarrow 1$  as well as when  $L$  increases.

Analytical predictions are compared to numerical simulations in Fig. 6. One observes that the approximate expression derived from Eq. (15) manages to describe the exponential cutoff in all cases and the scaling regime in the limit  $p \rightarrow 1$ , although it fails to predict the  $-3/2$  power-law neatly observed in numerical simulations for  $0 < p < 1$  as  $L \rightarrow \infty$  (notice in the lower panel of Fig. 6 the deviation for  $\tau \lesssim L$ , leading to a spurious power-law exponent  $-2$ ). This is due to the fact that the aging regime is overlooked by this approximation. Let us remark that a  $-3/2$  exponent is also found in classical queuing models with fluctuating length [3, 5] and the return time distribution of a random walk is at its origin. In view of the difficulties to find the exact expression for  $P_w(\tau)$ , to explain this scaling regime, we will solve next a closely related problem.

#### IV. AVALANCHES

Let us also consider now the events between two successive times when the number  $n$  of priorities above a given threshold  $x$  vanishes (avalanche). Avalanche duration is relevant in the present context as soon as it provides the duration of intervals in which there are queued tasks with priorities above a threshold to be executed. From the viewpoint of random walks, this is a first passage problem. Following the lines in Ref. [12], let us define  $Q_{n,t}(x)$ , the probability of having  $n$  values with priorities higher than  $x$ , given that an avalanche started at  $t = 0$  ( $t$  time units ago).  $Q_{n,t}$  follows the same ME (1)-(2) as  $P_{n,t}$  does, except for  $M_{0,1} = 0$ , and the initial condition is  $Q_{1,0} = 1 - x$  and  $Q_{n,0} = 0$ ,  $\forall n > 1$ . Thus, the probability that an avalanche, relative to threshold  $x$ , has duration  $t$  is

$$q_t(x) = xQ_{1,t-1}(x). \quad (20)$$

Fig. 7 illustrates the scaling that comes up for any  $p$  at the critical threshold  $x = 1 - p$ . Exact results were obtained by numerical integration of the ME for  $Q_n$  and compared to the results of numerical simulations of the BQM. Notice that the scaling region increases with  $L$  and shifts towards larger times as  $p \rightarrow 1$ .

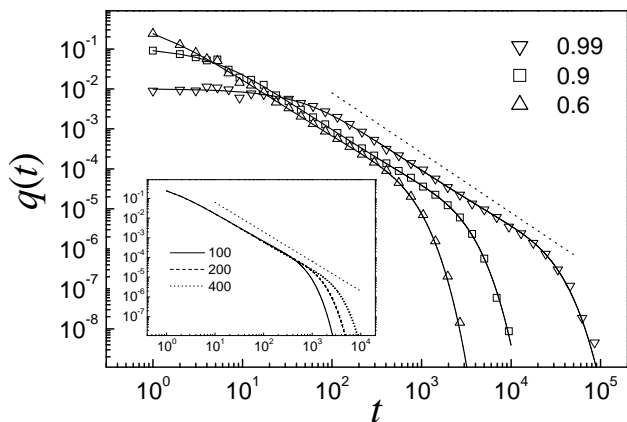


FIG. 7: Distribution of avalanche size  $q(t) \equiv q_t(x = 1 - p)$  for  $L = 100$ , different values of  $p$  indicated on the figure and  $R(x) = x$ . Solid lines join the exact values and symbols correspond to numerical simulations of the BQM. In the inset, exact results for  $p = 0.6$  and different values of  $L$  indicated on the figure are displayed. Dotted straight lines with slope  $-3/2$  are drawn for comparison.

The ME of  $Q_n$  can be solved analytically through diverse standard methods [13, 14]. Yet, in the limit of large  $L$  and fixed  $n$ , the ME describes a simple biased random walk, with an absorbing boundary at  $n = 0$  and probabilities to step either to the right, to the left, or remain still, given by  $m^+ = (1 - p)(1 - x)$ ,  $m^- = px$ ,  $m^0 = 1 - m^+ - m^-$ , respectively. From this viewpoint,  $q_t(x)$  is the probability that the first return to the origin occurs at  $t$  when the avalanche started at  $t = 0$ , while  $Q_{1,t}(x)$  is the probability of reaching  $n = 1$  at time  $t - 1$ , without having visited  $n \leq 0$ . Thus,  $q$  just differs from  $Q_1$  in appending the last step from 1 to 0. For any  $n$ ,  $Q_{n,t}(x)$  can be found by solving first the unbounded problem and then resorting to the reflection principle [15, 16]. Moreover, if we are concerned with the asymptotic behavior, we can directly take advantage of the Gaussian approximation from the central limit theorem. Therefore, one has

$$Q_{n,t}(x) \simeq (1 - x) \frac{e^{-\frac{(n-1-ct)^2}{2\sigma^2 t}} - \frac{m^-}{m^+} e^{-\frac{(n+1-ct)^2}{2\sigma^2 t}}}{\sqrt{2\pi\sigma^2 t}}, \quad (21)$$

where  $c$ , and  $\sigma^2$  are the mean and variance of each single step. This readily leads to the asymptotic behaviors

$$q_t(x) \sim \begin{cases} t^{-3/2}, & \text{if } c = 0 \\ t^{-1/2} \exp(\frac{-c^2 t}{2\sigma^2}), & \text{otherwise,} \end{cases} \quad (22)$$

that is, an exponential decay dominates the long-time decay in the biased cases, meanwhile, if  $c \equiv m^+ - m^- = 0$  (hence  $x = 1 - p$ ), a power-law arises in the large  $L$  limit, in agreement with the results displayed in Fig. 7 and with the well known results for a driftless random walk [16]. In particular, there is a correspondence with

the random annealed Bak-Sneppen model, where the same scaling is observed for any  $K$  at the critical threshold  $x = 1/K$  [12]. Let us remark that in the Bak-Sneppen model the transition matrix for the associated ME has  $2K$  non-null diagonals, and a generic univoque relation between  $p$  and  $K$  does not emerge. However, concerning avalanches, the equivalence between both models arises for  $K = 1/(1-p)$ . Due to the threshold being an upper or lower bound in each case, that relation is complementary to  $K = 1/p$  which arises by identifying ratios of deterministic/random sites [1].

## V. FINAL COMMENTS

Summarizing, we obtained analytical results for the BQM with queues of arbitrary length. Exact expressions were shown to be in agreement with the outcomes of numerical simulations of the dynamics. Progress has still

to be made to obtain the exact waiting time distribution that displays different regimes between the purely exponential one (at  $p = 0$ ) and the power-law decay with unit exponent (at  $p \rightarrow 1$ ), when  $L \rightarrow \infty$ . However, an approximate expression has been found that accounts for most of the distribution traits. Moreover, we have shown that avalanches, at the critical threshold  $x = 1-p$ , constitute another scale-free feature of the BQM for  $p > 0$ . Besides the main applications here illustrated, the present results may allow to estimate many other relevant statistical quantities of the BQM and can be extended to other queuing systems. Furthermore, our exact results set the basis to further explore the correspondence between BQM and other related models.

**Acknowledgements:** C.A. acknowledges D.R. Chialvo and R.O. Vallejos for useful suggestions and discussions, and Brazilian agencies CNPq and Faperj for partial financial support.

- 
- [1] A. Vazquez, J.G. Oliveira, Z. Dezso, K.I Goh, I. Kondor, A.-L. Barabási, *Phys. Rev. E* **73**, 036127 (2006).
  - [2] T. Nakamura, K. Kiyono, K. Yoshiuchi, R. Nakahara, Z.R. Struzik, Y. Yamamoto, *Phys. Rev. Lett.* **99**, 138103 (2007).
  - [3] A.-L. Barabási, *Nature* **435**, 207 (2005), and online supplementary information.
  - [4] P. Blanchard and M.-O. Hongler, *Phys. Rev. E* **75**, 026012 (2007).
  - [5] G. Grinstein, R. Linsker, *Phys. Rev. Lett.* **97**, 130201 (2006).
  - [6] A. Vazquez, *Phys. Rev. Lett.* **95**, 248701 (2005).
  - [7] D.O. Cajueiro, W.L. Maldonado, *Phys. Rev. E* **77**, 035101(R) (2008).
  - [8] A. Gabrielli, G. Caldarelli, *Phys. Rev. Lett.* **98**, 208701 (2007).
  - [9] A. Gabrielli, G. Caldarelli, *Phys. Rev. E* **79**, 041133 (2009).
  - [10] P. Bak, K. Sneppen, *Phys. Rev. Lett.* **71**, 4083 (1993).
  - [11] H. Flyvbjerg, K. Sneppen, P. Bak, *Phys. Rev. Lett.* **71**, 4087 (1993).
  - [12] J. de Boer, B. Derrida, H. Flyvbjerg, A.D. Jackson, T. Wettig, *Phys. Rev. Lett.* **73**, 906 (1994).
  - [13] W. Feller, *An introduction to probability theory and its applications* (John Wiley & Sons, New York, 1957).
  - [14] S. Redner, *A guide to first-passage processes* (Cambridge University Press, New York, 2001).
  - [15] M. Khantha, V. Balakrishnan, *J. Stat. Phys.* **41**, 811 (1985).
  - [16] M.E. Fisher, *J. Stat. Phys.* **34**, 667 (1984).